Cent. Eur. J. Phys. • 8(3) • 2010 • 438-444
DOI: 10.2478/s11534-009-0115-8

VERSITA

Central European Journal of **Physics**

Photoionization cross section and refractive-index change of hydrogenic impurities in a CdS-SiO_2 spherical quantum dot

Research Article

Sait Yılmaz[1]*, Haluk Şafak[2], Recep Şahingoz[1], Mustafa Erol[1]

1 *Faculty of Literature and Sciences, Department of Physics, Bozok University, 66200 Yozgat, Turkey*

2 *Faculty of Literature and Sciences, Department of Physics, Selçuk University, 42075 Konya, Turkey*

Received 25 March 2009; accepted 3 July 2009

Abstract: In this study, we calculate the photoionization cross section and refractive-index change of an on-center hydrogenic impurity in a CdS-SiO_2 spherical quantum dot. In numerical calculations, both the finite- and infinite-confinement cases are considered and a variational scheme is adopted to determine the energy eigenvalues for the impurity. The variations of the photoionization cross section with the dot radius, the refractive-index change, and the normalized photon energy are investigated, and the effect of the potential-barrier height on the cross section is discussed. The results obtained show that the photoionization cross section and the refractive-index change in CdS-SiO_2 spherical quantum dots are sensitively dependent on the incident optical intensity and on the dot sizes.

PACS (2008): 71.55.Gs; 73.21.La; 78.67.Hc

Keywords: photoionization cross section • refractive-index change • hydrogenic impurities • quantum dots

1. Introduction

Rapid developments in modern epitaxial growth techniques have enabled researchers to create structures on the nanometer scale where many fascinating new physical phenomena have been discovered. Because of their reduced dimensionality, these nano-scaled structures show very unique properties for device applications, especially in laser and optoelectronic technology [1–12]. Therefore, great attention has been focused on the electronic and optical properties of these confined systems. Bastard [13, 14] was the first to deal with the problem of the binding energy of the hydrogenic impurity in a quantum well. Lee and Spector [15] have calculated the binding energy of an impurity in quantum wires in 1984. After that, a variational approach has been adopted to the hydrogenic impurity problem in a spherical quantum dot. This latter idea was pioneered by A.I. Ekimov *et al.* [16]. The binding energy of a hydrogenic impurity in a spherical quantum dot has been calculated by Zu *et al.* [17]. In recent years, several theoretical studies have advocated an approach concentrating on the binding energy of impurity states in spherical quantum dots for different confinement-potential shapes [18–24].

*E-mail: yilmazs@erciyes.edu.tr

The photoionization cross section and refractive-index changes play a fundamental role in understanding the optical properties of impurities in both semiconductor bulk materials and in heterostructures. The photoionization cross section of hydrogenic impurities in bulk semiconductors was investigated first by Lax [25]. Takikawa *et al.* [26] have examined the photoionization of deep traps in *AlGaAs/GaAs* multiple quantum wells. The dependence of the photoionization cross section on the photon energy in semiconductors for different impurity potentials has been investigated by Ilaiwi and Tomak [27]. Also, the effect of the well width [28] and the polarization direction of light [29] on the photoionization of impurities in both finite- and infinite-barrier quantum wells have been studied. In quantum-well wire structures, photoionization of impurities has been studied by Sali *et al.* [30]. In their works, the authors have taken into account a rectangular wire and considered both finite- and infinite-confinement cases. In a similar study, the photoionization cross section has been calculated for different potential heights in $Ga_{1-x}Al_xAs/GaAs$ heterostructures [31]. The variation of the photoionization with the dot radius for both on-center and off-center impurities in spherical quantum dots has been reported by Ham *et al.* [32, 33]. In addition to the above mentioned studies, the spectral dependence of the photoionization cross section in quantum box structures has been analyzed in Ref. [34]. Ham *et al.* [35] have investigated the photoionization in a cylindrical quantum wire using an infinite-well model.

The refractive index for intersubband optical transitions in the infinite confining potential regime in semiconductor quantum dots and its linear and nonlinear optical properties were discussed in Refs. [36–43]. In Refs. [44–46], the intersubband optical absorption coefficients and the refractive-index changes were calculated for a quantum box, a cylindrical quantum dot, and for the quantum dots of core-shell structures. However, there is no theoretical study on the photoionization cross section in the finite-well approximation and on the refractive-index changes of hydrogenic impurities in CdS-SiO_2 spherical quantum dots.

In this study, the photoionization cross section and refractive-index change associated with an on-center shallow donor impurity in a spherical CdS-SiO_2 quantum dot is investigated as a function of the dot radius and the normalized photon energy. Numerical calculations are performed for both finite- and infinite-confinement cases. The effect of the potential height on the cross section and on the refractive-index changes is discussed. In calculations, a variational scheme within an effective-mass approximation is used to determine the binding energy of the impurity.

2. Theory

The photoionization cross section can be defined as the ionization probability of electrons bound to a hydrogenic impurity under an external optical excitation, and therefore it should be strongly dependent on the confinement profile and its strength as well as on the excitation energies. An electron residing in the ground state of an impurity can undergo a transition to an excited state in the subband continuum by an interaction with incident electromagnetic radiation. In order for such a transition to occur, the excitation energy should be greater than the photoionization threshold energy E_s. As known from the literature, the photon energies involved in a photoionization process in small quantum dots (QDs) are generally larger than those for quantum wells (QWs) or quantum-well wires (QWWs) systems [34]. The main reason for this is the increase in the confinement of the electrons and thus the enhancement of the optical photoionization threshold energies.

The photoionization cross section of an impurity can be given in the well-known dipole approximation as

$$\sigma(\hbar w) = \left[\left(\frac{E_{eff}}{E_0}\right)^2 \frac{n_r}{\epsilon}\right] \frac{4\pi^2}{3}\, \alpha_{FS}\, \hbar w \sum_f |\langle\psi_i|\,\vec{r}\,|\psi_f\rangle|^2\ \delta(E_f - E_i - \hbar w). \quad (1)$$

Here, n_r is the optical refractive index of the material, ϵ is the dielectric constant of the medium, $\alpha_{FS} = (e^2/(4\pi\epsilon_0\hbar c))$ is the fine-structure constant, and (E_{eff}/E_0) is the so-called effective-field ratio that defines the ratio of the effective electric field of the incoming radiation and the average field in the medium. In real systems, it is difficult to calculate this ratio, but it has no effect on the shape of the photoionization cross section, and therefore it is taken as unity. In the above equation, $|\langle\psi_i|\,\vec{r}\,|\psi_f\rangle|^2$ is the squared dipole matrix element between an initial ψ_i state and a final ψ_f state; E_f and E_i are the final- and initial-state energies, respectively.

The model considered here is a system consisting of an electron bound to a shallow hydrogenic impurity in a spherical quantum dot. Within the effective-mass approximation, the Hamiltonian for such a system can be written as follows:

$$H = -\frac{\hbar^2}{2m^*}\nabla_r^2 - \frac{e^2}{4\pi\epsilon r} + \frac{\ell(\ell+1)\hbar^2}{2m^* r^2} + V(r). \quad (2)$$

Here, e is the electronic charge, m^* is the effective mass of the electron, and $V(r)$ is the confining potential. If $V(r)$

is chosen as infinite outside the spherical dot and zero inside it, *i.e.*,

$$V(r) = \begin{cases} 0, & r \le R, \\ \infty, & r > R, \end{cases}$$

then the eigenfunctions corresponding to the above Hamiltonian, in the presence of the impurity, can be given by following trial wave functions

$$\psi_{10}(r) = \begin{cases} N\, j_0(k_{10} r)\, e^{-\lambda r}, & r \le R, \\ 0, & r > R, \end{cases} \tag{3}$$

for the ground state and

$$\psi_{21}(r) = \begin{cases} M\, j_1(k_{21} r)\, e^{-\lambda r}, & r \le R, \\ 0, & r > R, \end{cases} \tag{4}$$

for the first excited state. Here, $j_l(k_{n\ell})$ are the spherical Bessel functions. In the above equations, N and M are normalization constants, λ is a variational parameter that has to be determined using the energy-minimization requirement, $k_{10} = \sqrt{2m^* E_{10}/\hbar^2}$, and $k_{21} = \sqrt{2m^* E_{21}/\hbar^2}$. On the other hand, if the $V(r)$ potential is chosen finite and constant outside the spherical dot and zero inside it such as

$$V(r) = \begin{cases} 0, & r \le R, \\ V_o, & r > R, \end{cases}$$

then the relevant eigenfunctions would have the form

$$\psi_{10}(r) = \begin{cases} N j_0(\kappa_{10} r) e^{-\lambda r}, & r \le R, \\ N \left(\frac{j_0(\kappa_{10} R)}{k_0(\chi_{10} R)} \right) k_0(\chi_{10} r)\, e^{-\lambda r}, & r > R, \end{cases} \tag{5}$$

for the ground state and

$$\psi_{21}(r) = \begin{cases} M j_1(\kappa_{21} r) e^{-\lambda r}, & r \le R, \\ M \left(\frac{j_1(\kappa_{21} R)}{k_0(\chi_{21} R)} \right) k_0(\chi_{21} r)\, \frac{R}{r} \left(\frac{1+\chi_{21} r}{1+\chi_{21} R} \right) e^{-\lambda r}, & r > R, \end{cases} \tag{6}$$

for the first excited state. In a similar manner, $\kappa_{10} = \sqrt{2m_1^* \xi_{10}/\hbar^2}$, $\kappa_{21} = \sqrt{2m_1^* \xi_{21}/\hbar^2}$, $\chi_{10} = \sqrt{2m_2^*(\xi_{10} - V_o)/\hbar^2}$ and $\chi_{21} = \sqrt{2m_2^*(\xi_{21} - V_o)/\hbar^2}$. Here, m_1^* and m_2^* are the electron effective masses inside and outside the spherical CdS quantum dot, respectively. The binding energy of the hydrogenic impurity can be evaluated as

$$E_b(R, r) = \frac{\hbar^2 k_{n\ell}^2}{2m^*} - E_{\min}(R, r). \tag{7}$$

Here, $E_{\min}(R, r)$ is calculated by minimizing the matrix element $\langle \psi_{n\ell} \mid H \mid \psi_{n\ell} \rangle$ with respect to the variational parameter λ for each dot radius R.

In the calculation of the photoionization cross section, we have used a narrow Lorentzian instead of the δ-function in Eq. (1):

$$\delta(E_f - E_i - \hbar\omega) = \frac{\hbar\Gamma}{\pi \left[(\hbar\omega - (E_f - E_i))^2 + (\hbar\Gamma)^2 \right]}. \tag{8}$$

Here, Γ is the hydrogenic impurity linewidth; it is taken to be sufficiently small, so that it has very little effect on the shape of the total photoionization cross-section profile. The linear and the third-order nonlinear refractive-index changes can be defined as [44]

$$\frac{\Delta n^{(1)}(\omega)}{n_r} = \frac{1}{2 n_r^2 \varepsilon_0} |M_{21}|^2 \sigma_V \left[\frac{E_{21} - \hbar\omega}{(E_{21} - \hbar\omega)^2 + (\hbar\Gamma_{12})^2} \right], \tag{9}$$

$$\frac{\Delta n^{(3)}(\omega)}{n_r} = -\frac{\mu c}{4 n_r^3 \varepsilon_0} |M_{21}|^2 \frac{\sigma_V I}{\left[(E_{21} - \hbar\omega)^2 + (\hbar\Gamma_{12})^2 \right]^2} \times \Bigg[4(E_{21} - \hbar\omega) |M_{21}|^2 - \frac{(M_{22} - M_{21})^2}{E_{21}^2 + (\hbar\Gamma_{12})^2} \Big\{ (E_{21} - \hbar\omega) \times \left[E_{21}(E_{21} - \hbar\omega) - (\hbar\Gamma_{12})^2 \right] - (\hbar\Gamma_{12})^2 (2E_{21} - \hbar\omega) \Big\} \Bigg], \tag{10}$$

where n_r is the refractive index, σ_V is the carrier density in this system, μ is the permeability of the system, ϵ_R is the real part of the dielectric constant, Γ_{ij} denotes the relaxation rate, E_{ij} is the energy interval between two different electronic states, I is the incident optical intensity, and M_{ij} is the matrix element defined by $M_{ij} = |\langle \psi_i | qx | \psi_j \rangle|$.

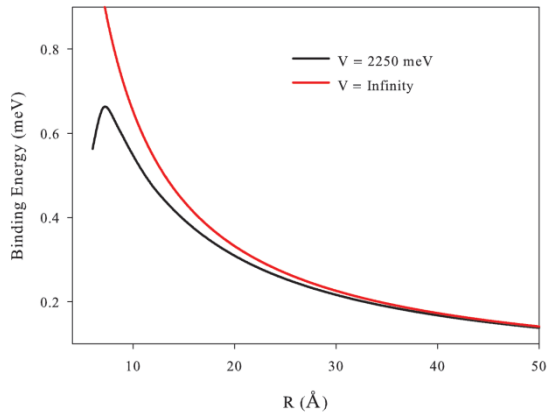

Figure 1. The variation of binding energy with the dot radius in a CdS quantum dot for infinite and $V = 2250$ meV confinement potential.

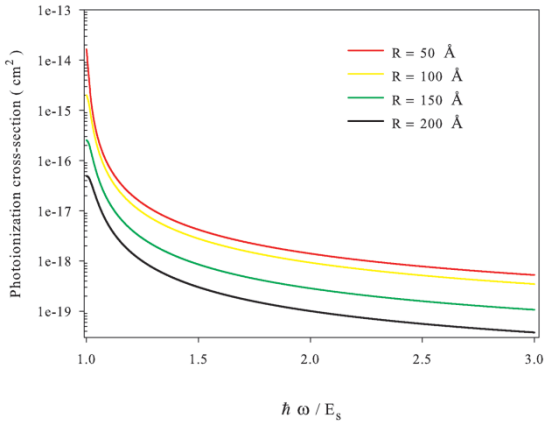

Figure 2. The photoionization cross section as a function of the normalized photon energy in a CdS quantum dot for the infinite-confinement case.

Then, the total refractive-index change is given by

$$\frac{\Delta n(\omega)}{n_r} = \frac{\Delta n^{(1)}(\omega)}{n_r} + \frac{\Delta n^{(3)}(\omega)}{n_r}. \qquad (11)$$

3. Results and discussions

In our numerical calculations, we have used reduced atomic units such that $\hbar = m_0 = e = 1$. In accordance with these units, the effective Bohr radius is given by $a^* = \hbar^2\epsilon/(m^*e^2)$ and the effective Rydberg energy is $R^* = m^*e^2/(2\hbar^2\epsilon^2)$. The material parameters are $a^* = 16.17$Å, $m^* = 0.18m_0$, $\epsilon = 5.5$, the band gap energy is 2.5 eV, and $n_r = 2.5$ for CdS [47]. On the other hand, $m^* = 0.916m_0$, $\epsilon = 4$, and the band gap energy is 7 eV for the barrier material Silica glass [48].

The binding energies of hydrogenic impurities in a CdS-SiO_2 quantum dot have been calculated within the effective-mass approximation by using the variational method. The variation of the binding energy with the dot radius has been plotted for the infinite and $V = 2250$ meV confinement case in Fig. 1. From this figure, it can be seen that the binding energy decreases with increasing dot radius for both confinement cases, as expected. There is an apparent peak in the curve for the finite-confinement case of $V = 2250$ meV at a certain small dot radius at which the binding becomes maximal.

In Fig. 2, the variations of the photoionization cross section with the normalized photon energy for a shallow impurity for four different dot radii have been plotted in the infinite- confinement case. It can be seen from this figure that the photoionization cross section is decreasing with increasing normalized photon energy for all dot radii. This

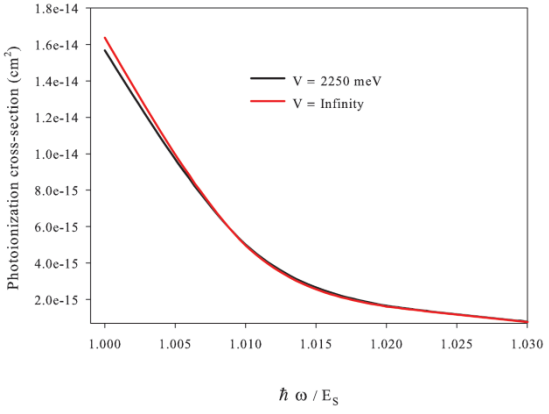

Figure 3. The photoionization cross section as a function of the normalized photon energy in a CdS quantum dot for the infinite and $V = 2250$ meV confinement case ($R = 50$ Å).

decrease is stronger at large dot radii than at small ones. On the other hand, when the normalized photon energies approach unity, there are sharp rises in all curves, which points at a resonance situation.

To compare the finite- and infinite-confinement cases near the resonance situation, we have calculated the photoionization cross section as a function of the normalized photon energy at a constant dot radius of 50 Å, and the results are given in Fig. 3. The variations of photoionization cross sections with the photon energy are very close to each other for both cases in a wide region. The distinction between them becomes significant only for values of the normalized energy that lie near the resonance condition of unity. Therefore, we can conclude from this behavior that the confinement strength is important only near the resonance for a certain dot radius, and as we go away

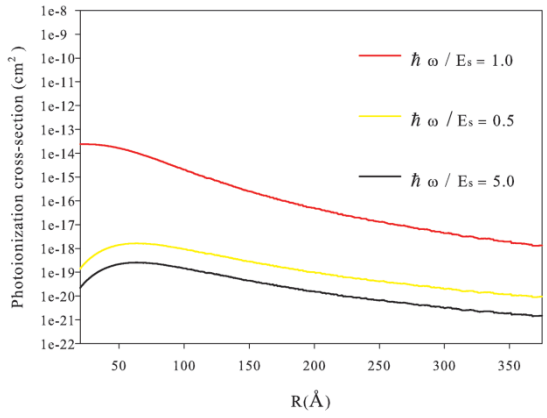

Figure 4. The photoionization cross section as a function of the dot radius for three different normalized photon-energy values in a CdS quantum dot in the infinite-confinement case.

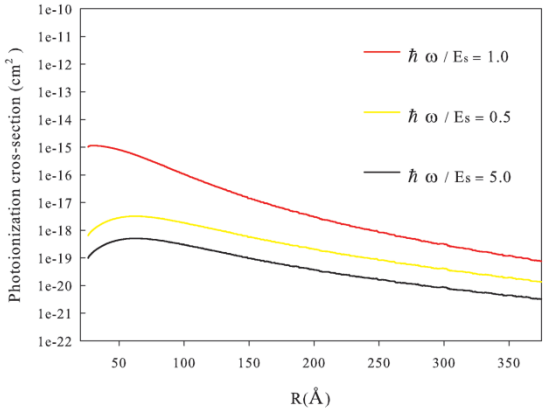

Figure 5. The photoionization cross section as a function of the dot radius for three different normalized photon-energy values in a CdS quantum dot in the $V = 2250$ meV confinement case.

from the resonance, the effect of confinement on the photoionization cross section would become less important.

In Figs. 4 and 5, we have plotted the variation of the photoionization cross section with the dot radius for three different normalized photon energies for the infinite confinement and 2250 meV potential height cases, respectively. As seen from these figures, the curves that correspond to the off-resonant cases increase smoothly with decreasing dot radius until a certain small dot-radius value; thereafter they decrease more rapidly. Namely, there is a certain dot-radius value at which the photoionization reaches its maximum. But the curves corresponding to the resonant case do not show such a turning point, and the photoionization cross section approaches a constant value when the radius is further decreased. Another point to be noticed is that the magnitudes of the photoionization cross section for the resonant case are significantly larger than those for both of the off-resonant cases over the whole range of dot radii, which is an expected feature. This result is more apparent for the infinite-confinement case. At smaller dot radii, the distinction between the resonant and the off-resonant cases becomes greater for both finite and infinite confinement.

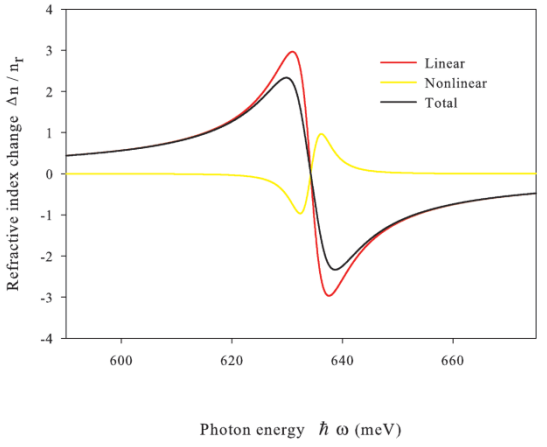

Figure 6. The variation of the linear, third-order, and total refractive-index change with the photon energy in the infinite-confinement case ($R = 20$ Å, $I = 4$ MW/cm^2).

Besides the photoionization cross section of CdS quantum dots embedded into a SiO_2 matrix, we have also investigated the linear and nonlinear refractive-index changes of these structures. For this purpose, we have calculated the linear, third-order, and total refractive-index changes as a function of the photon energy, and the results are given in Fig. 6. In the calculations of these variations, the values used for the dot radius and the incident optical intensity are 20 Å and 4 MW/cm^2, respectively. Also, the infinite-well approximation is assumed. In the vicinity of the resonance energy, the common behaviors of the curves are found to be in agreement with expectations. To investigate the dependence of the total refractive-index change on the incident optical intensity, we have calculated the variations of the total refractive-index change with the photon energy for four different optical intensities of $I = 0, 2, 4$, and 6 MW/cm^2, and the results are plotted in Fig. 7. As can be seen in this figure, the incident optical illumination has reduced the magnitude of the total refractive-index change. This is due to the further enhancement of the nonlinear (third-order) refractive-index change with the optical intensity. Since the linear refractive index is independent of the intensity (see Eq. (9)), an increase in the optical illumination has no effect on the linear part of the refractive index. On the other hand, the

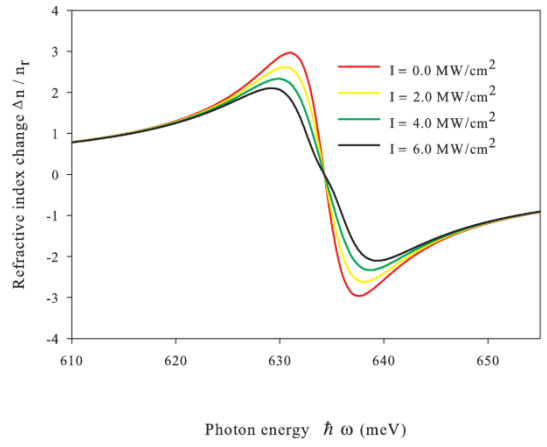

Figure 7. The variation of the total refractive-index change with the photon energy for four different optical intensities in the infinite-confinement case ($R = 20$ Å).

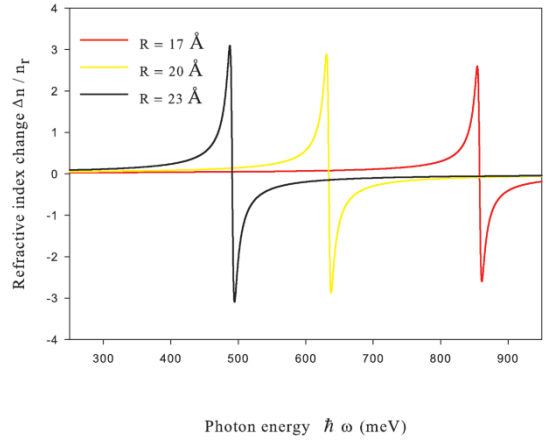

Figure 8. The variation of the total refractive-index changes with the photon energy for three different radii in the infinite-confinement case ($I = 0.45$ MW/cm^2).

nonlinear part depends directly on the illumination, and so increasing the intensity enhances the magnitude of the third-order refractive index. Since these two parts are opposite in sign, the overall effect is the reduction of the total refractive-index change with the optical intensity.

Finally, we have calculated the variation of the total refractive-index change with the photon energy for three different dot radii. The results are given in Figs. 8 and 9 for the infinite- and finite-confinement cases, respectively. Here, the optical intensity is taken as $I = 0.45$ MW/cm^2. By inspecting these two figures, one can see immediately the strong red-shift behavior for the refractive-index resonance with increasing dot radius. For example, in the case of infinite confinement (Fig. 8), the resonance peak

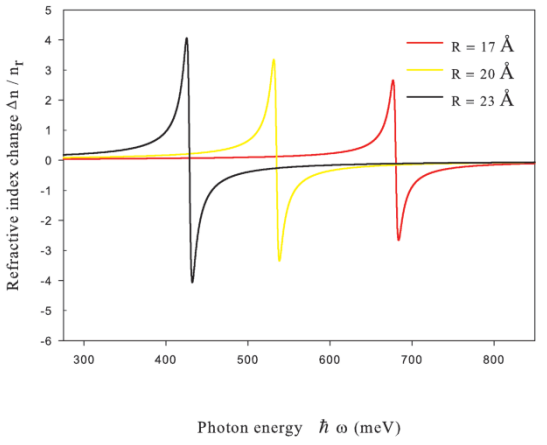

Figure 9. The variation of the total refractive-index changes with the photon energy for three different radii in the $V = 2250$ meV confinement case ($I = 0.45$ MW/cm^2).

has been shifted towards smaller energies from approximately 850 meV to about 480 meV by increasing the dot radius by only 6 Å. A similar red shift is observed also for the finite-confinement case, as is seen in Fig. 9. Another important result that can be extracted from these two figures is the effect of confinement on the resonance-peak positions. For a given dot-radius value, the peak position is shifted towards lower energies with decreasing confinement. Therefore, we can conclude that the maximum resonance energy at the total refractive-index change for any specific dot-radius value occurs in the infinite-confinement situation. In other words, one can claim a yellow shift for the refractive-index maximum with increasing confinement. These two parameters, the dot radius and the confinement strength, permit us to adjust precisely the resonance conditions and hence many optical properties related to it in any optical system using these materials.

4. Conclusions

In this study, we have investigated the photoionization cross section and the refractive-index change of an on-center hydrogenic impurity in a CdS-SiO_2 spherical quantum dot. Both the photoionization and the total refractive-index change including the third-order (nonlinear) contribution are important quantities in understanding the optical properties of any bulk material or heterostructure. The results obtained here demonstrate a strong dependence of these physical quantities on the dot radii and illumination strength for the cases of infinite and finite barrier height. In addition, red shift with the dot size or blue shift with the confinement strength in the refractive-index change

together can allow us to tune the resonance frequencies as desired. In tuning the optical properties more precisely, the incident optical intensity can also be used as another parameter. We believe that this study will be beneficial to get more information about the optical properties of these kinds of structures.

Acknowledgements

This work is partly supported by the BAP office of Selçuk University.

References

[1] M. A. Reed, Sci. Am. 268, 118 (1993)
[2] N. Kristaedter et al., Appl. Phys. Lett. 69, 1226 (1996)
[3] E. Leobandung, L. Guo, S. Y. Chou, Appl. Phys. Lett. 67, 2338 (1995)
[4] K. K. Likharev, IBM J. Res. Dev. 32, 1444 (1998)
[5] D. Loss, D. P. Divicenzo, Phys. Rev. A 57, 120 (1998)
[6] X. Jiang, S. S. Li, M. Z. Tidrow, Physica E 5, 27 (1999)
[7] P. A. Sundqvist, V. Narayan, J. Vincent, M. Willander, Physica E 15, 27 (2002)
[8] M. Grundmann, Physica E 5, 167 (2000)
[9] M. Shin, S. Lee, K. W. Park, G.-H. Kim, Solid State Commun. 116, 527 (2000)
[10] S. Y. Wang, S. D. Lin, H. W. Wu, C. P. Lee, Infrared Phys. Techn. 42, 473 (2001)
[11] A. Perera, Opto-Electron. Rev. 14, 99 (2006)
[12] A. Perera et al., Opto-Electron. Rev. 15, 223 (2007)
[13] G. Bastard, Surf. Sci. 113, 165 (1982)
[14] G. Bastard, Phys. Rev. B 24, 4714 (1983)
[15] J. Lee., H. N. Spector, J. Vac. Sci. Technol. B 2, 16 (1984)
[16] A. I. Ekimov, Al. L. Efros, M. G. Ivanov, A. A. Onushchenko, S. K. Shumilov, Solid State Commun. 69, 565 (1989)
[17] J. L. Zu, J. J. Xiong, B. L. Gu, Phys. Rev. B 41, 6001 (1990)
[18] C. M. Hsiao, W. N. Mei, D. S. Chuu, Solid State Commun. 81, 807 (1992)
[19] G. Murillo, N. Porras-Montenegro, Phys. Status Solidi B 220, 187 (2000)
[20] V. Ranjan, Vijay A. Singh, J. Appl. Phys. 89, 6415 (2001)
[21] C. Bose, C. K. Sarkar, Phys. Status Solidi B 218, 461 (2000)
[22] S. Yılmaz, H. Şafak, Physica E 36, 40 (2007)
[23] M. El Assaid, M'hamed El Aydi, M. El Feddi, F. Dujardin, Cent. Eur. J. Phys. 6, 97 (2008)
[24] S. Yılmaz, H. Şafak, Int. J. Mod. Phys. B 23, 2127 (2009)
[25] M. Lax, In the Proceeding of the 1954. Atlantic City Conference on Photoconductivity (Wiley, New York, 1956) 111
[26] M. Takikawa, K. Kelting, G. Brunthaler, M. Takechi, J. Komeno, J. Appl. Phys. 65, 3937 (1989)
[27] K. F. Ilaiwi, M. Tomak, J. Phys. Chem. Solids 51, 361 (1990)
[28] M. E. Said, M. Tomak, J. Phys. Chem. Solids 52, 603 (1991)
[29] M. I. Kawni, M. Tomak, Surf. Sci. 260, 319 (1992)
[30] A. Sali, M. Fliyou, H. Satori, H. Loumrhari, Phys. Status Solidi B 211, 661 (1999)
[31] A. Sali, M. Fliyou, H. Loumrhari, Physica B 233, 196 (1997)
[32] H. Ham, H. N. Spector, J. Appl. Phys. 93, 3900 (2003)
[33] H. Ham, C. J. Lee, J. Korean Phys. Soc. 42, 688 (2003)
[34] A. Sali, H. Satori, M. Fliyou, H. Loumrhari, Phys. Status Solidi B 232, 209 (2002)
[35] H. Ham, C. J. Lee, H.N. Spector, J. Appl. Phys. 96, 335 (2004)
[36] M. Şahin, Phys. Rev. B 77, 045317-1 (2008)
[37] B. Liu et al., Int. J. Mod. Phys. B 15, 1959 (2001)
[38] T. Takagahara, Phys. Rev. B 36, 9293 (1987)
[39] T. Brunhes et al., Phys. Rev. B 61, 5562 (2000)
[40] İ. Karabulut, S. Ünlü, H. Şafak, Phys. Status Solidi B 242, 2902 (2005)
[41] S. Sauvage et al., Phys. Rev. B 59, 9830 (1999)
[42] L. Liu, J. J. Li, G. G. Xiong, Physica E 25, 466 (2005)
[43] C. Z. Zhang, K. X. Guo, Z. E. Lu, Physica E 36, 92 (2007)
[44] S. Ünlü, İ. Karabulut, H. Şafak, Physica E 33, 319 (2006)
[45] Cui-Hong Liu, Bai-Ru Xu, Phys. Lett. A 372, 888 (2008)
[46] Xi Zhang, Guiguang Xiong, Xiaobo Feng, Physica E 33, 120 (2006)
[47] G. T. Einevoll, Phys. Rev. B 45, 3410 (1992)
[48] J. Sée, P. Dollfus, S. Galdin, J. Appl. Phys. 92, 3141 (2002)